Recrystallization Behavior of CoCrCuFeNi High-Entropy Alloy

AUTHOR(S):

Park, Nokeun; Watanabe, Ikuto; Terada, Daisuke; Yokoyama, Yoshihiko; Liaw, Peter K.; Tsuji, Nobuhiro

CITATION:

Park, Nokeun ...[et al]. Recrystallization Behavior of CoCrCuFeNi High-Entropy Alloy. Metallurgical and Materials Transactions A 2014, 46(4): 1481-1487

ISSUE DATE:

2014-10-08

URL:

http://hdl.handle.net/2433/200193

Title:

Recrystallization behavior of CoCrCuFeNi high-entropy alloy

Authors:

Nokeun Park[1], Ikuto Watanabe[1], Daisuke Terada[1,2], Yoshihiko Yokoyama[3], Peter K. Liaw[4], Nobuhiro Tsuji[1,5]*

Affiliation:

[1]Department of Materials Science and Engineering, Kyoto University, Yoshida Honmachi, Sakyo-ku, Kyoto 606-8501, Japan

[2]Department of Mechanical Science and Engineering, Chiba Institute of Technology, Tsudanuma, Narashino, Chiba 275-0016, Japan

[3]Institute for Materials Research, Tohoku University, Sendai, Miyagi 980-8577 Japan

[4]Department of Materials Science and Engineering, The University of Tennessee, Knoxville, TN 37996-2100, USA

[5]Elements Strategy Initiative for Structural Materials (ESISM), Kyoto University, Yoshida Honmachi, Sakyo-ku, Kyoto 606-8501, Japan

Contact:

*Corresponding author:

Email: nobuhiro-tsuji@mtl.kyoto-u.ac.jp

Tel: +81-75-753-5462

Fax: +81-75-753-4978

Email addresses for all authors:

park.nokeun.22x@st.kyoto-u.ac.jp

watanabe.ikuto.57a@st.kyoto-u.ac.jp

daisuke.terada@p.chibakoudai.jp

yy@imr.tohoku.ac.jp

pliaw@utk.edu

nobuhiro-tsuji@mtl.kyoto-u.ac.jp

Abstract:

We investigated recrystallization behavior of a cold-rolled CoCrCuFeNi high-entropy alloy (HEA). Two different face-centered cubic phases having different chemical compositions and lattice constants existed in the as-cast specimen have different chemical compositions: one phase was the Cu-lean matrix and the other was the Cu-rich second phase. The second phase remained even after a heat treatment at 1100°C and Cu enriched more in the Cu-rich second phase. The calculated mixing enthalpies of both Cu-lean and Cu-rich phases in the as-cast and heat-treated specimens explained that Cu partitioning during the heat treatment decreased the mixing enthalpy in both phases. In the specimens 90% cold-rolled and annealed at 650°C, 700°C and 800 °C, recrystallization proceeded with increasing the annealing temperature, and ultrafine recrystallized grains with grain sizes around 1 μm could be obtained. The microhardness tended to decrease with increasing the fraction recrystallized, but it was found that the microhardness values of partially recrystallized specimens were much higher than those expected by a simple rule of mixture between the initial and cold-rolled and specimens. The reason for the higher hardness was discussed based on the ultrafine grain size, sluggish diffusion expected in HEAs, and two phase structure in the CoCrCuFeNi alloy.

Keywords:

High-entropy alloy (HEA), CoCrCuFeNi, cold-rolling, recrystallization, grain refinement

1 Introduction

In metallurgy it is general to design a new alloy by selecting one major element and considering small amounts of alloying elements, in order to achieve certain properties. Such a traditional way has enlarged our understanding about various effects of small amounts of additional elements in metallic materials. In 2004, on the other hand, Cantor et al. designed new alloys which consisted of 5 to 20 elements with equiatomic percent where there was no longer major element unlike conventional alloys previously designed [1]. Many researchers have studied such multi-elements alloys composed of nearly equiatomic compositions, which often show single-phase solid solution and are named as *high-entropy alloys* (HEAs) [2–9] [10].

HEAs have been attracting more and more attentions, since they often show superior mechanical properties, such as high strength, large strain-hardening capabilities, high fracture toughness, and so on [5–9]. By now, however, most studies on HEAs carried out in laboratory scales have dealt with as-cast materials or those just after simple homogenization heat treatment. Similar to conventional metals and alloys, there would be a great possibility of microstructural control through thermomechanical processing in HEAs, for improving their properties much more. Because low diffusivity is expected in HEAs [3,10] fine and thermally stable grain structures are expected to be realized. In this study, we have focused on clarifying deformation and recrystallization behaviors of a HEA.

One critical issue in the field of HEAs is how to predict which phases exist in a given composition. There are no reliable phase diagrams for multi-elementary HEAs. In case of binary alloys, Hume-Rothery theory based on difference in atomic size, electron concentration, electronegativity and relative valence, is well known for predicting the solubility [11], but it is unclear whether the same procedures are applicable to HEAs

including large concentration of many elements. It has been, however, reported that two factors, i.e., mixing enthalpy (ΔH^{mix}) and atomic size difference (δ), are dominant to predict the phase stability in a given HEA composition [4,5,11,12]. According to previous reports [4], CoCrFeNiMn, CoCrCuFeNi and CoCrFeNiV alloys are predicted to show single solid-solutions without any intermetallic compounds. There are a few reports about recrystallization behaviors of CoCrFeNiMn [6,7,13], but recrystallization studies in CoCrCuFeNi and CoCrFeNiV alloys have not been carried out yet. In the present study, therefore, we study on recrystallization behaviors of CoCrCuFeNi HEA through conventional cold-rolling and subsequent annealing heat-treatment.

2. Experimental Procedures

The material used in the present study was an equimolar CoCrCuFeNi alloy (20 mol.% for each element) that was cast with the pseudo float melting process which brings almost homogeneous distribution of each element [14]. An as-cast HEA rod 10 mm in diameter and 60 mm in length was homogenized at 1100 °C for 12 hours, followed by water cooling. A specimen 4.6 mm long was cut from the homogenized rod, and rolled by 90 % reduction in thickness at room temperature to obtain a sheet specimen 0.46 mm thick. The cold-rolled specimen was annealed at 600, 650, 700 and 800 °C for 1.8, 3.6 and 7.2 ks. Microstructures of the cold-rolled and annealed specimens were observed by a field-emission scanning electron microscope (SEM) with backscattered electron (BSE) and electron back-scattering diffraction (EBSD) detectors. Chemical composition at local areas in the specimens was measured by using energy-dispersive X-ray spectroscopy (EDS) in SEM. For the microstructural observations, cross-sections perpendicular to the rolling direction (RD) of the cold-rolled and annealed specimens were mechanically polished, and then electro-polished in a solution of 10% $HClO_4$ and 90% CH_3COOH at 25 °C. The recrystallized grain sizes in the annealed specimens were measured by a mean linear intercept method on BSE-SEM images. Phase identification was carried out by the use of X-ray diffraction (XRD) patterns using Cu-Kα at 45 kV and 40 mA. Vickers hardness test was also carried out, using a load of 9.8 N and duration time of 10 s.

3. Results and discussion

Phase analysis of the alloy

SEM microstructure of the as-cast specimen are shown in **Fig. 1**. The specimen shows a dendrite structure, and two different regions (possibly different phases) with different contrasts are observed in **Fig. 1**. EDS analysis was carried out in two regions shown in **Fig.1b**, and it was shown that two regions had different chemical concentrations as summarized in **Table 1**. Major difference between two regions is copper content. The region with dark contrast (zone 1) is Cu-lean, while Cu is enriched in the region with white contrast (zone 2). The XRD pattern of the as-cast specimen shown in **Fig. 2** indicates that there are two different phases having the same face-centered cubic (FCC) structure but different lattice parameters, 0.36148 nm and 0.35859 nm. As the area fractions of Cu-rich and Cu-lean regions in **Fig. 1** are 0.23 and 0.77, respectively, the Cu-rich and Cu-lean phases should have the lattice parameters of 0.36148 nm and 0.35859 nm, respectively. It is considered, therefore, that Cu is discharged from the primarily solidified phase (dark phase in **Fig. 1**) and enriched to form another Cu-rich phase. There seem no peaks corresponding to superlattice diffractions in **Fig. 2**, which suggests both FCC phases are solid solution. If so, it is quite curious that two different solid solution phases having the same crystal structure co-exist in the solidified structure.

The as-cast specimen was homogenized at 1100°C for 12 hrs, and SEM microstructures of the homogenized specimen are shown in **Fig. 3**. After the homogenization treatment, coarse matrix grains having mean grain size of 350 μm are observed instead of dendrite structure, as shown in **Fig. 3a**. The coarse grains presumably correspond with solidified grains with identical orientations. Even after the homogenization treatment, phase separation was still observed. The cu-rich phase having white contrast was spheroidized

and coarsened, as shown in **Figs. 3a** and **b**. It is interesting that the Cu-rich phase exhibits really a spherical shape (**Fig. 3b**). Hardness changed from 162 HV of the as-cast specimen into 139 HV of the heat-treated specimen. The chemical concentrations of two regions in the homogenized specimen, indicated as zones 3 and 4 in **Fig. 3a**, are shown in **Table 2**. Compared with the as-cast specimen (**Table 1**), the difference in Cu-concentration between the Cu-rich phase and the Cu-lean phase rather increased by the heat treatment. When we consider the chemical mixing enthalpy in binary systems composed of two elements included in the present alloy, it may be possible to explain the observed phase separation. **Table 3** represents the chemical mixing enthalpy, ΔH_{mix} (kJ mol^{-1}), in the binary systems among Co, Cr, Cu, Fe and Ni. The chemical mixing enthalpies between Cu and other elements always show positive values, while other combinations have zero or negative values of mixing enthalpy. This suggests that Cu atoms have repulsive interactions with other four elements and tend to form Cu-Cu bonding in terms of enthalpy, which seems to correspond qualitatively with the result of phase separation in the present alloy. A consideration of mixing enthalpy has been also adapted to multi-elementary HEAs [9,11,12,15]. Equation 1 describes how to obtain the empirical mixing enthalpy in a given HEA [9,11,12].

$$\Delta H^{mix} = 4 \sum_{i=1, j\neq i}^{N} \Delta H_{AB}^{mix} c_i c_j \qquad (1)$$

where ΔH^{mix} is the predicted mixing enthalpy of the system, N is the number of elements involved in the alloy, ΔH_{AB}^{mix} is the mixing enthalpy of binary system consisting of elements i^{th} and j^{th}, and c_i is the atomic percent of i^{th} element. The calculated mixing enthalpies in the Cu-rich phase in both as-cast and homogenized specimens are +3.1 and +2.2 kJ mol^{-1} which are much higher than those of the Cu-lean phase in two specimens (**Table 4**). The

reason of Cu partitioning during the heat treatment is reasonable in terms of reducing the mixing in this alloy system.

Cold-rolling and Recrystallization

Figure 4 shows SEM-BSE images of the specimens cold-rolled to 90% reduction in thickness. Hardness increased from 139 HV of the 1100 °C heat-treated specimen to 330 HV by the 90% cold-rolling. Gray areas are the Cu-lean phase, and black areas are the Cu-rich phase. Both Cu-rich and Cu-depleted phases are elongated to RD, and deformation structures are developed in the Cu-lean matrix. **Figure 5** represents SEM-BSE images of the specimens 90% cold-rolled and subsequently annealed at various temperatures from 600 °C to 800 °C for 1.8 ks. Recrystallized microstructures could be distinguished in the Cu-lean matrix, while no substructures can be seen in the darkly etched Cu-rich phase. The value of mean microhardness and the area fraction recrystallized (f_{rex}) are presented in **Fig. 5** as well. The specimen annealed at 600 °C seemed not to be recrystallized in the present study since the annealing temperature might be too low for the occurrence of recrystallization. When the annealing temperature was higher than 650 °C, however, some recrystallized grains having different contrasts, i.e., different crystallographic orientations, appeared as shown in **Figs. 5b-c**, and the area fraction recrystallized increased with increasing temperature. As a result, the value of microhardness decreased with increasing annealing temperature. Based on those results, it is possible to determine the recrystallization temperature of CoCrCuFeNi alloy that is in between 600 and 650 °C. This range is close to one-half of the melting temperature of CoCrCuFeNi alloy in Kelvin that Tong et al. reported the melting temperature of the present alloy which is approximately 1380 °C [16].

In order to understand deformation and recrystallization microstructures of the Cu-lean matrix more in details, EBSD orientation analysis was conducted. **Figure 6** shows inverse pole figure maps of the specimens 90% cold-rolled and then annealed at various temperatures for different periods. Colors in the maps indicate crystallographic orientation parallel to RD, according to the key steregraphic triange shown in the figure. Low angle boundaries with misorientation of 2° to 15°, high angle boundaries with misorientation above 15° and Σ3 twin boundaries are drawn in blue, black and red lines, respectively. The matrix of the specimen annealed at 600 °C for 7.2 ks (**Fig. 6a**) contained almost low-angle boundaries and the color within each elongated matrix gradually varied, indicating that the matrix had deformation microstructures partially recoveried but unrecrystallized even after 7.2 ks annealing. This result implies that temperature 600 °C is below the recrystallization temperature of this alloy. However, the specimen annealed at 650 °C (**Fig. 6b**) showed different microstructural features. Although deformation microstructures partially existed still, but large fraction of recrystallized grains were clearly seen in **Fig. 6b**. Fraction of high-angle boundaries including twin boundaries within the matrix was 0.59, indicating that recrystallization considerablely progressed. The area fraction recrystallized obtained from the EBSD result was 0.62. **Figure 6c** shows the specimen annealed at 700 °C for 1.8 ks. Upper region was almost recrystallized, but lower region showed unrecrystallized deformation microstructures including small portion of recrystallization. Such a big difference suggests an orientation dependence of recrystallization in this alloy. **Figure 6d** shows an EBSD map of the specimen annealed at 800 °C for 1.8 ks. Most of the matrix areas were covered by recrystallized grains, although there were still small portin of unrecrystallized regions. The fraction of high-angle boundaries including twin boundaries was 0.86. It is noteworthy that the fraction of twin boundaries in **Fig. 6d** is 0.45, indicating that the stacking fault energy

(SFE) of the matrix is fairly low in the alloy. It is known that low-stacking fault energy of {111} planes inhibits dynamic recovery during plastic deformation, leading to high dislocation densities, i.e., large driving force for recrstallization, in the deformed materials. It is also interesting that most of annealing twins are aligned parallal to the normal direction (ND) of the rolled specimen and are linked to the Cu-rich phase. It is reported that one outstanding feature of HEAs is a sluggish diffusion [3,10]. Such a sluggish diffusion of atoms would inhibit growth of recrystallized grains, maintaning finer grain sizes during annealing process. For example, the mean grain sizes of the recrystallized regions in **Figs. 6c** and **d** are 1.0 and 1.4 μm, respectively, which are ultrafine grain szes. According to Hall-Petch relationship, such a fine grain size would enhance strength of the material.

Figure 7 shows the change in average microhardness of the specimens annealed at different temperatures for various periods as a function of the fraction recrystallized. Open square, open circle and open triangle indicate the results of the specimens annealed at 650, 700 and 800 °C, respectively. Solid diamond and solid hexagon are the hardness of the specimens heat-treated at 1100 °C (fraction of recrystallization, f_{rex}, is 100%) and subsequently cold-rolled by 90% reduction (f_{rex} = 0%), respectively. Under an assumption that microhardness is proportionally decreased with increasing the fraction recrystallized, i.e., a linear rule of mixture, a dash-dotted line is drawn between the homogenized specimen (solid diamond) and the cold-rolled one (solid hexagon), according to the equation. 2.

$$HV_{mix} = f_{rex} HV_h + (1 - f_{rex}) HV_d \qquad (2)$$

where HV_h and HV_d are microhardness values of the homogenized specimen (139 HV) and the cold-rolled one (330 HV), respectively. As the fraction recrystallized increases, the microhardness value decreases as expected. However, it is clearly seen that the values of microhardness of the partially recrystallized specimens are much higher than the value

expected by the rule of mixture, which seems interesting since the hardness of the deformed matrix should rather decrease due to recovery process during annealing. One of the possible reasons for the higher hardness of the partially recrystallized specimens is the mean grain size of the recrystallized area. It is well known from Hall-Petch relationship that strength of metallic materials increases as mean grain size of microstructure decreases. As seen in **Figs. 5** and **6**, the grain size of the recrystallized regions in the present alloy was fairly fine. For instance, the mean grain sizes of the specimens annealed at 650, 700 and 800 °C for 1.8 ks are 0.7, 1.0 and 1.4 μm, respectively. Such a fine grain size in the partially recrystallized specimen might maintain high hardness even after recrystallization. It is interesting to discuss the reasons why such ultrafine-grained microstructure is obtained in the present study. One reason must be a sluggish diffusion in HEAs. It has been reported that the normalized activation energy (Q/T_m, where Q is the activation energy (kJ mol^{-1}) for substitutional diffusion in a given alloy, T_m is the melting temperature with an unit of Kelvin) of individual element in HEAs is higher than the normalized activation energy of self-diffusion in pure metals of the elements. Another reason for the fine grain size might be related to the fact that the current alloy consists of two phases. Grains having different lattice parameters and chemical concentrations are elongated after cold-rolling, as shown in **Fig. 4**, to result in channels with small thickness. During subsequent annealing, grain growth toward ND of recrystallized grains in one phase is interrupted by the other phase. Such an anisotropic grain growth during annealing might result in keeping ultrafine-grained structure. So far, there are several unclear things in the present alloy. For example, many pits were observed in the Cu-lean phase after partial recrystallization, as shown in **Fig. 5**, which suggests precipitation of another phase. If fine precipitation happens, it would increase the hardness of the alloy and keep fine grain sizes of the matrix. Further systematic research on detailed

microstructure evolution as well as data collection of diffusivity of the alloy is necessary for deepening understanding of the possibilities of microstructure control in the present alloy.

4. Summary and conclusion

In the present investigation, we studied recrystallization behaviors of conventionally cold-rolled CoCrCuFeNi HEA, and discussed its microstructure evolution and hardness changes. The major results obtained are listed as follows:

1. The as-cast specimen had a dendrite structure consisting of two different FCC phases. The Cu-lean matrix and Cu-rich phase formed between solidified dendrites had lattice parameters of 0.35859 nm and 0.36148 nm, respectively.
2. After a heat treatment at 1100 °C, the two phase structure maintained. The Cu-rich phase was spheroidized, and the dendrite structure disappeared. Enrichment of Cu in the Cu-rich phase rather proceeded by the heat treatment.
3. Cu had positive mixing enthalpy with other four elements in binary combinations. We calculated the empirical mixing enthalpies of both Cu-depleted and Cu-rich phases in the as-cased and homogenized specimens. The results supported the Cu enrichment during the heat treatment, as the mixing enthalpy of both Cu-rich and Cu-lean phase increased by partitioning of Cu.
4. Fine grain sizes around 1 μm were obtained in the Cu-lean matrix after recrystallization. After 90% cold-rolling and subsequent annealing, microhardness tended to decrease with increasing the fraction recrystallized. However it was found that the hardness of the partially recrystallized specimens was much higher than the value expected by a rule of mixtures between the 1100 °C heat-treated and cold-rolled specimens. The higher hardness and fine recrystallized grain size in the present alloy were discussed together.

Acknowledgement

This study was financially supported by the Grant-in-Aid for Scientific Research on Innovative Area, ‘‘Bulk Nanostructured Metals’’ (Area No.2201), the Grant-in-Aid for Scientific Research (A) (No.24246114), the Grant-in-Aid for Challenging Exploratory Research (No.26630365), and the Elements Strategy Initiative for Structural Materials (ESISM), all through the Ministry of Education, Culture, Sports, Science and Technology (MEXT), Japan (Contact No. 22102002). N.P. was supported also by the Japan Society for Promotion of Science (JSPS) as a JSPS postdoctoral fellow. All the support is grate- fully appreciated.

References

[1] B. Cantor, I.T.H. Chang, P. Knight, and A.J.B. Vincent: Mater. Sci. Eng. A, 2004, vol. 375-377, pp. 213–18.

[2] J.-W. JW Yeh, S.-K. SK S.-K. Chen, S.-J. SJ S.-J. Lin, J.-Y. Gan, T.-S. Chin, T.-T. Shun, C.-H. Tsau, and S.-Y. Chang: Adv. Eng. Mater., 2004, vol. 6, pp. 299–303.

[3] Jien-Wei Yeh: JOM, 2013, vol. 65, pp. 1759–71.

[4] Kuibao Zhang and Zhengyi Fu: Intermetallics, 2012, vol. 22, pp. 24–32.

[5] Michael C. Gao: JOM, 2013, vol. 65, pp. 1749–50.

[6] W.H. Liu, Y. Wu, J.Y. He, T.G. Nieh, and Z.P. Lu: Scr. Mater., 2013, vol. 68, pp. 526–29.

[7] F. Otto, a. Dlouhý, Ch. Somsen, H. Bei, G. Eggeler, and E.P. George: Acta Mater., 2013, vol. 61, pp. 5743–55.

[8] M.J. Yao, K.G. Pradeep, C.C. Tasan, and D. Raabe: Scr. Mater., 2014, vol. 72-73, pp. 5–8.

[9] Yong Zhang, Ting Ting Zuo, Zhi Tang, Michael C Gao, Karin A Dahmen, Peter K Liaw, and Zhao Ping Lu: Prog. Mater. Sci., 2014, vol. 61, pp. 1–93.

[10] K.-Y. Tsai, M.-H. Tsai, and J.-W. Yeh: Acta Mater., 2013, vol. 61, pp. 4887–97.

[11] Y. Zhang, Y. J. Zhou, J. P. Lin, G. L. Chen, and P. K. Liaw: Adv. Eng. Mater., 2008, vol. 10, pp. 534–38.

[12] Akira Takeuchi and Akihisa Inoue: Mater. Trans. JIM, 2000, vol. 41, pp. 1372–78.

[13] P.P. Bhattacharjee, G.D. Sathiaraj, M. Zaid, J.R. Gatti, Chi Lee, Che-Wei Tsai, and Jien-Wei Yeh: J. Alloys Compd., 2014, vol. 587, pp. 544–52.

[14] Y Yokoyama, K Inoue, and K Fukaura: Mater. Trans., 2002, vol. 43, pp. 2316–19.

[15] F. Otto, Y. Yang, H. Bei, and E.P. George: Acta Mater., 2013, vol. 61, pp. 2628–38.

[16] Chung-jin Tong, Yu-Liang Chen, Jien-wei Yeh, Su-jien Lin, Swe-kai Chen, Tao-tsung Shun, Chun-huei Tsau, and Shou-yi Chang: Metall. Mater. Trans. A, 2005, vol. 36, pp. 881–93.

Figure Captions

Figure 1 SEM micrographs of the as-cast specimen of CoCrCuFeNi. The local areas where EDS measurement was carried out are marked as zone 1 and zone 2 in (b).

Figure 2 X-ray diffraction pattern of the as-cast specimen of CoCrCuFeNi.

Figure 3 SEM microstructures after homogenization treatment at 1100 °C for 12 hrs. The areas where EDS measurement was carried out are marked as zone 3 (Cu-lean) and zone 4 (Cu-rich) in (a).

Figure 4 SEM-BSE images of the specimen cold-rolled to 90% reduction. Gray areas are the Cu-lean phase, and black areas are the Cu-rich phase.

Figure 5 SEM-BSE microstructures of the specimens 90% cold-rolled and then annealed at various temperatures for 1.8 ks.

Figure 6 EBSD inverse pole figure maps of the specimens 90% cold-rolled and then annealed at various temperatures for different periods. Low angle boundaries with misorientation (θ) of 2° to 15°, the high angle boundaries with misorientation above 15°, and Σ3 twin boundaries are drawn in blue, black and red lines, respectively.

Figure 7 Mean microhardness of the specimens 90% cold-rolled and then annealed at different temperatures as a function of the fraction recrystallized.

Table 1 Chemical concentrations (atomic percent) in two local regions shown in Fig. 1b of the as-cast specimens measured by EDS in SEM.

Table 2 Chemical concentrations (atomic percent) in two local regions shown in Fig. 3a of the homogenized specimens measured by EDS in SEM.

Table 3 Chemical mixing enthalpy, ΔH_{mix} (kJ mol^{-1}), in binary systems composed of two elements included in the present alloy.

Table 4 Calculated mixing enthalpy, ΔH_{mix} (kJ mol^{-1}), of each zone shown in Tables 1 and 2, according to Eq. 1.

Figure 1 SEM micrographs of the as-cast specimen of CoCrCuFeNi. The local areas where EDS measurement was carried out are marked as zone 1 and zone 2 in (b).

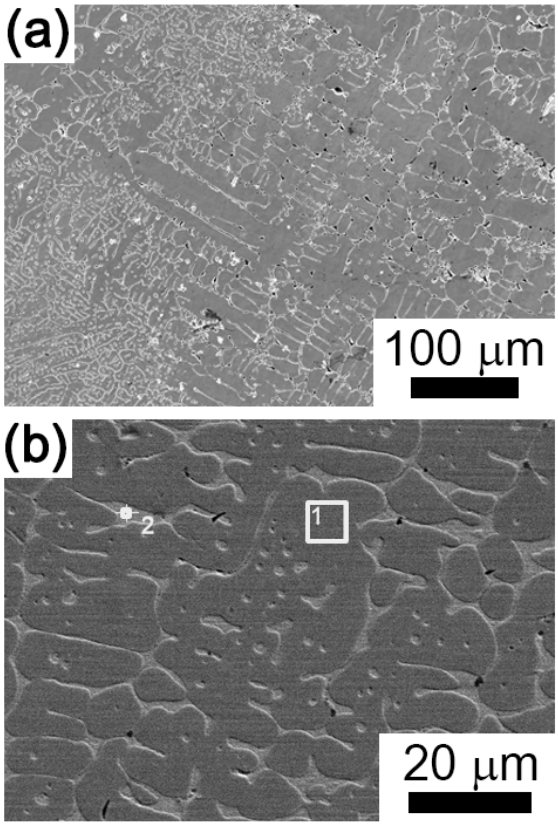

Figure 2 X-ray diffraction pattern of the as-cast specimen of CoCrCuFeNi.

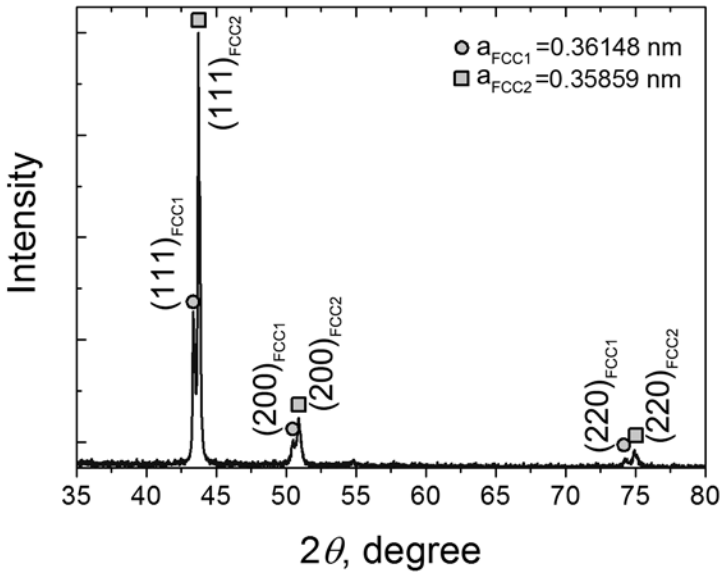

Figure 3 SEM microstructures after homogenization treatment at 1100 °C for 12 hrs. The areas where EDS measurement was carried out are marked as zone 3 (Cu-lean) and zone 4 (Cu-rich) in (a).

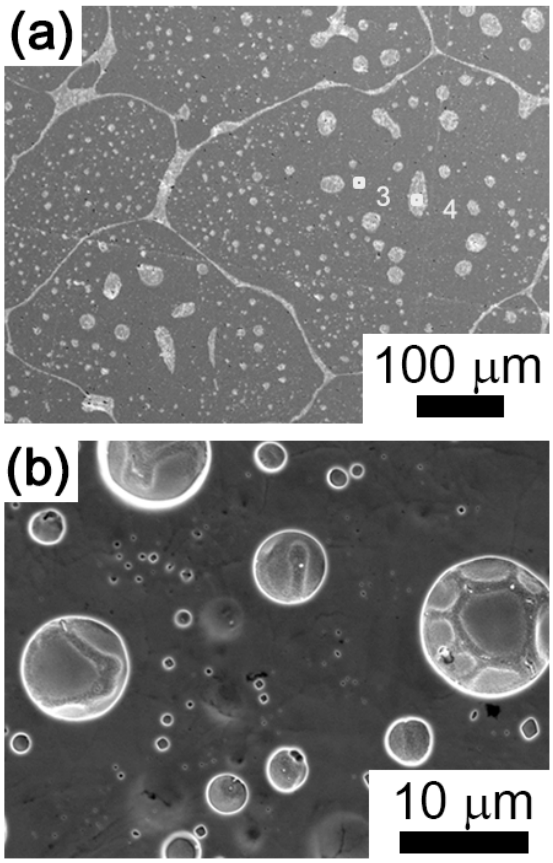

Figure 4 SEM-BSE images of the specimen cold-rolled to 90% reduction. Gray areas are the Cu-lean phase, and black areas are the Cu-rich phase.

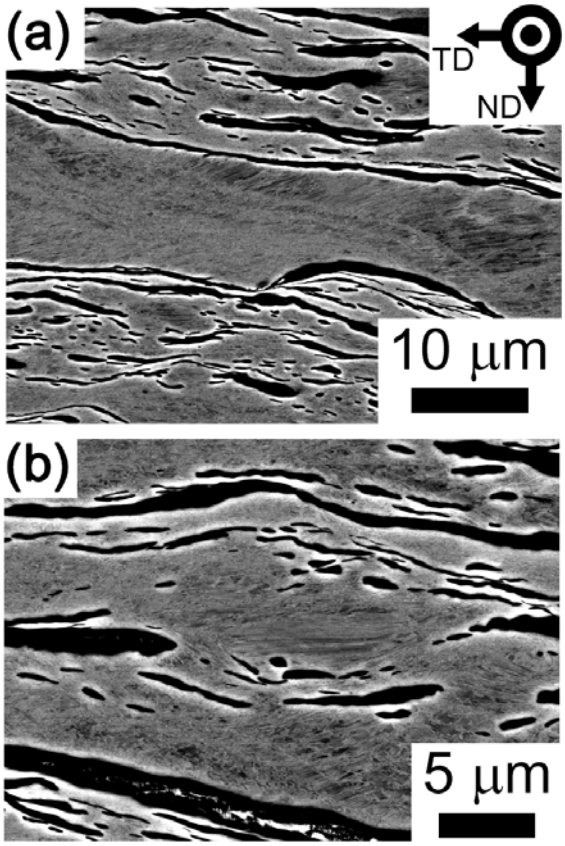

Figure 5 SEM-BSE microstructures of the specimens 90% cold-rolled and then annealed at various temperatures for 1.8 ks.

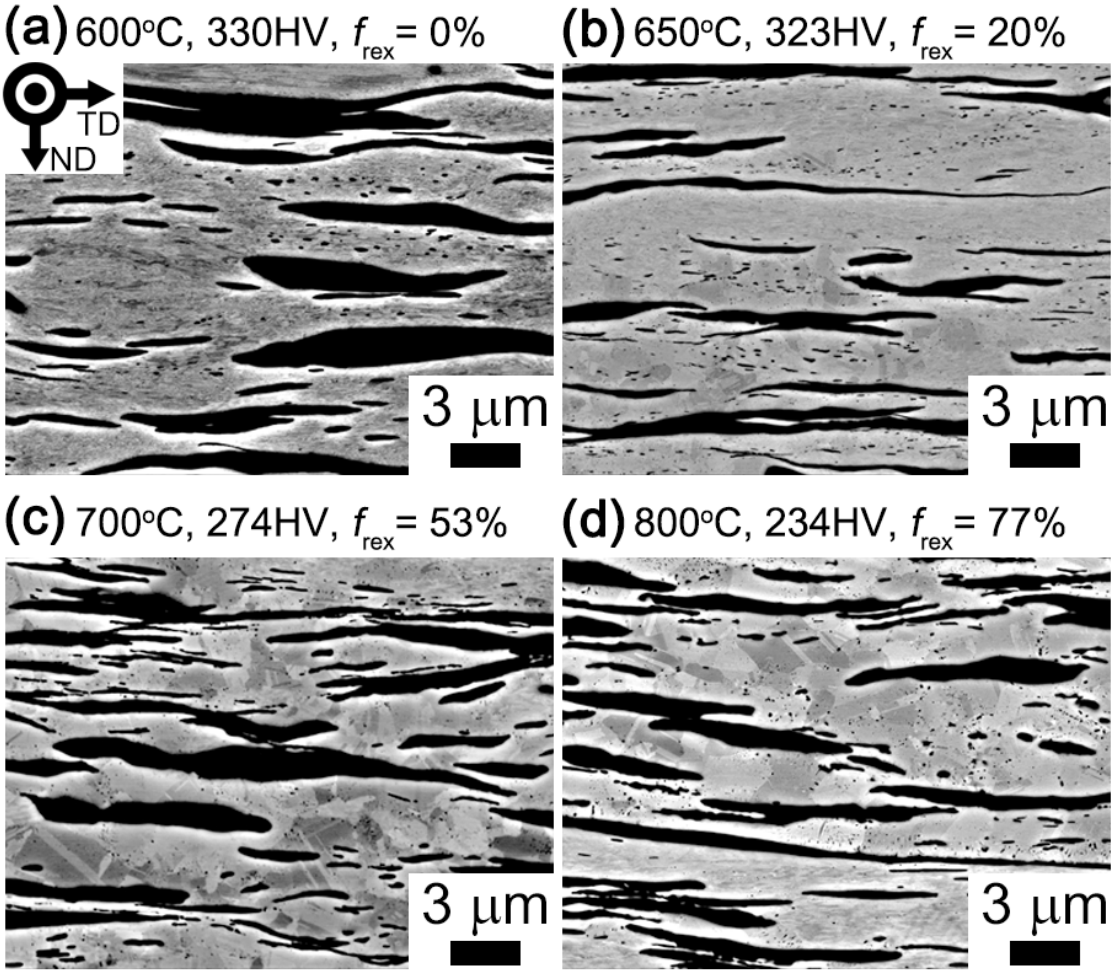

Figure 6 EBSD inverse pole figure maps of the specimens 90% cold-rolled and then annealed at various temperatures for different periods. Low angle boundaries with misorientation (θ) of 2° to 15°, the high angle boundaries with misorientation above 15°, and Σ3 twin boundaries are drawn in blue, black and red lines, respectively.

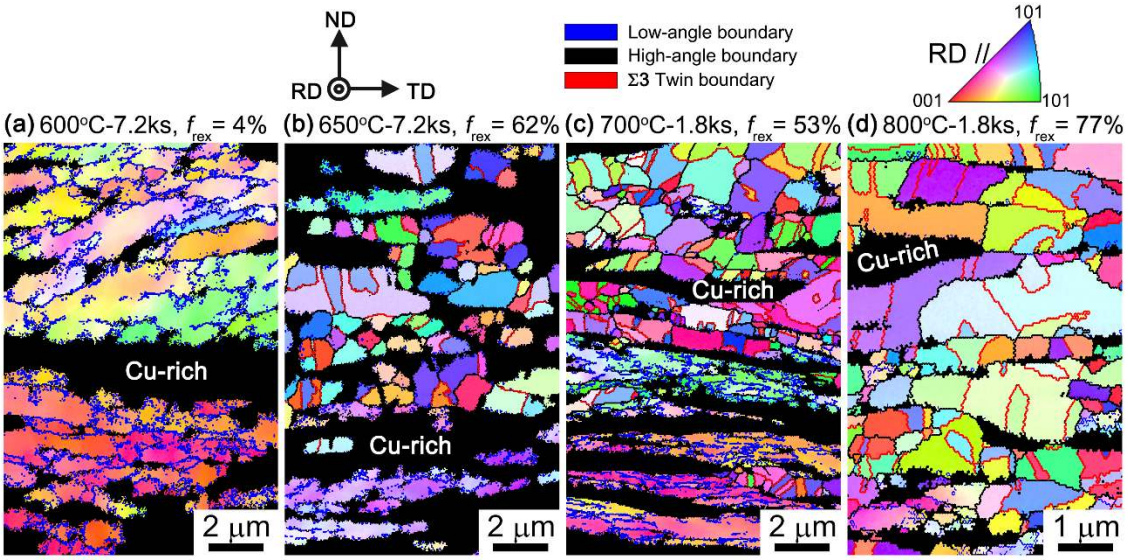

Figure 7 Mean microhardness of the specimens 90% cold-rolled and then annealed at different temperatures as a function of the fraction recrystallized.

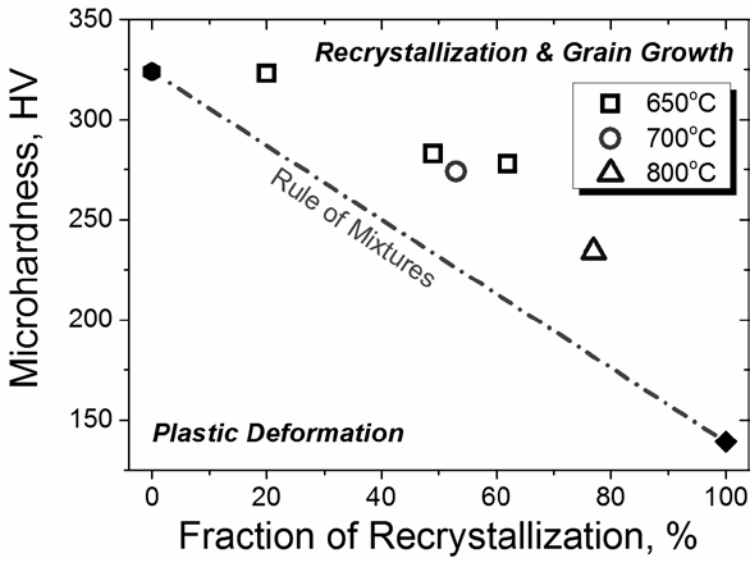

Table 1 Chemical concentrations (atomic percent) in two local regions shown in Fig. 1b of the as-cast specimens measured by EDS in SEM.

Specimen	Zone	Co	Cr	Cu	Fe	Ni
As-cast	No. 1	24.2	25.4	**9.4**	26.2	14.8
	No. 2	3.0	3.6	**85.7**	3.4	4.3

Table 2 Chemical concentrations (atomic percent) in two local regions shown in Fig. 3a of the homogenized specimens measured by EDS in SEM.

Specimen	Zone	Co	Cr	Cu	Fe	Ni
Homogenized	No. 3	25.27	24.74	**7.72**	25.44	16.82
	No. 4	2.15	2.69	**90.19**	1.98	2.99

Table 3 Chemical mixing enthalpy, ΔH_{mix} (kJ mol^{-1}), in binary systems composed of two elements included in the present alloy.

	Co	Cr	Cu	Fe	Ni
Co	-	-4	+6	-1	0
Cr	-	-	+12	-1	-7
Cu	-	-	-	+13	+4
Fe	-	-	-	-	-2
Ni	-	-	-	-	-

Table 4 Calculated mixing enthalpy, ΔH_{mix} (kJ mol^{-1}), of each zone shown in Tables 1 and 2, according to Eq. 1.

Specimen	Zone	ΔH_{mix}
As-cast	No. 1 (Cu-lean)	+1.0
	No. 2 (Cu-rich)	+3.1
Homogenized	No. 3 (Cu-lean)	+0.4
	No. 4 (Cu-rich)	+2.2